Proceedings of 7th National Conference on Wind Engineering (VII-NCWE)

Nov 21-22, 2014

Editors :
Dr. Naveen Kwatra,
Dr. Shruti Sharma
Dr. Dwarikanath Ratha

ORGANIZED BY :

THAPAR UNIVERSITY

DEPARTMENT OF CIVIL ENGINEERING
THAPAR UNIVERSITY PATIALA

ISWE

INDIAN SOCIETY FOR WIND ENGINEERING

Proceedings of the 7th National Conference on "Wind Engineering (VII-NCWE)

November 21-22, 2014

Organized by

Department of Civil Engineering

Thapar University, Patiala

and

Indian Society for Wind Engineering

Sponsored by

Technical Education Quality Improvement Programme (TEQIP)

Building Materials & Technology Promotion Council (BMTPC)

Skeleton/ESCOM Consultants Pvt. Ltd.

Infrastructure Leasing & Financial Services Limited (IL&FS)

New "Full"-scale Wind and Wind-driven-rain Testing Approaches for Wind Damage Mitigation

G.T. Bitsuamlak[a]
[a] Civil and Environmental Engineering/WindEEE Research Institute,
University of Western Ontario (UWO), London, ON, Canada, N6A 5B9
Presenting authors email: gbitsuam@UWO.ca

Abstract

The wind and wind-driven-rain performance of buildings depends on climate conditions, aerodynamics of the building and its surroundings, fine exterior architectural elements, construction material (and details). This paper discusses the emerging multi-scale testing methods that are suitable to investigate the wind and wind-driven-rain performance of buildings and its appurtenances. Two such facilities are the Wall of Wind at Florida International University and the WindEEE Dome at UWO whose unique features are described in this paper. Notably WindEEE Dome produces tornadic flows in addition to other types of wind systems. For relatively small sized study cases such as low-rise buildings or building appurtenances, study models that are fabricated with the actual construction materials following commonly used construction practices and reproducing finer architectural details on the exterior of the building are used. This results in a high resolution wind load information not only on the building structural system, or large cladding components such as roof systems, walls etc., but also on both sides of individual tiles, roof pavers and roof top equipment/solar panels etc., where failures usually initiates and cascades to other parts of the building. In addition, it also allows realistic assessment of the effects of architectural elements, openings, and construction material and details on the wind-driven-rain performance and opens the door for related wind mitigation technology developments. For large sized study cases such as tall buildings, it allows testing at 1:100 or 1:200 scaled models, i.e. quadruple times than typical scales, at higher wind speed. This alleviates the Reynold's number similarity discrepancies, for example seen with curved cornered buildings, and fine façade architectural detail related issues, for example screen walls, while testing in small and low-wind speed testing facilities. Application examples on full-scale and high resolution evaluation of wind load on tiles with various profiles, roof pavers, and roof mounted appurtenances such as roof top equipment and solar panels are discussed. Recently developed wind-driven-rain simulation method that generates rain-drop-size distributions similar to those encountered in tropical storms together with its application for studies on WDR deposition on low-rise building and water intrusion through various roof secondary water barriers are presented.

Key words: Wall of Wind, WindEEE Dome, Wind load, Wind-driven-rain, Hurricane, Tornado, Building, Solar Panel, Roof Top Equipment, Tile, Roof Paver, Wind Damage Mitigation

1. Introduction

Maintaining civil infrastructure's resiliency against natural hazards (e.g. typhoon) is necessary to sustain safety and prosperity of communities. Exposure to wind hazards has significantly increased due to higher activities in coastal regions. Recent typhoon in Hayan, Philippines cost 7500 lives and caused billions of dollars in damage. In North America Hurricane Andrew in 1992 caused $26.5 billion in damage in Florida. Katrina in 2005 caused $108 billion in damage. The inland is also affected by high intensity local storms (non-synoptic winds) such as tornadoes and downbursts that cause the majority of insured property losses due to natural catastrophes. According to Munich Re America, the five-year average insured loss due to thunderstorm activity (tornados and downbursts) in North America is of the order of $6 billion.

Significant progress has been made in (i) experimental atmospheric boundary layer (ABL) flows and their impacts on generic bluff bodies, buildings and structures and components (e.g. Castillo et al., 2004; Bitsuamlak et al.,

2009; Gan Chowdhury et al., 2010; Kopp et al., 2011; Liu et al., 2013, Aly et al. 2012 and Tecle et al. 2013); (ii) non-synoptic wind systems (Holmes et al., 2008; Haan et al., 2008; Mishra et al. 2008a and b; Matsui et al. 2009; Hashemi-Tari et al., 2010; Hangan 2014) and computational wind engineering (Selvam et al., 2003; Bitsuamlak et al., 2005; Kim and Hangan, 2007; Tamura et al., 2008; Natarajan and Hangan, 2012; Dagnew and Bitsuamlak, 2013; Abdi and Bitsuamlak 2014, Dagnew and Bitsuamlak 2014, Nasir et al. 2014, Nasir and Bitsuamlak 2014, Aboshosha et al. 2014). The boundary layer wind tunnel (BLWT) has become an industry wide accepted tool, but used only for straight-line winds (Cochran 2006). Recently, several full-scale experimental approaches have been (or are being) developed that are capable of testing building models with actual construction materials at large-scale and high wind speeds (Bitsuamlak et al., 2009; Hangan 2014; Kopp et al., 2011; Liu et al., 2013;). Small and large scale experimental facilities for tornadic wind flows are also becoming available (Haan et al., 2008; Mishra et al. 2008a and b; Xu and Hangan, 2008; Matsui et al. 2009; Hashemi-Tari et al., 2010 Rajasekharan et al. 2012). Recent analysis has shown that the characteristics of tornados and downbursts differ significantly from those of straight large scale winds (Nasir et al. 2014).

Although significant progress has been made in experimental wind engineering, there are notable gaps in large-scale testing and non-synoptic wind studies such as tornado and downburst. With wide interest in sustainable building design there is also a gap on the climate modeling for the sustainable built-environment. Typical BLWTL are designed with medium to tall buildings applications as target and therefore can accurately reproduce ABL flows at scale between 1/50 and 1/800. Very low rise structures or ground based devices (such as solar panels) will lay bellow the ABL height properly reproduced in BLWT's (Aly and Bitsuamlak 2013). Building appurtenances scaled down with the scale of large buildings will loses the resolution required to maintain the aerodynamic requirements (for example roof tile profiles disappear and typical wind tunnel models test smooth roofs, roof top equipment's becomes too small to instrument etc.).

Important gaps in experimental and numerical characterization of tornadoes and downbursts clearly exist and their interaction with the built environment is the least understood (Letchford et al., 2002; Holmes et al., 2008; Hangan, 2014; van de Lindt, 2012). Most existing experimental/numerical simulations based on non-tornado, non-downburst wind models may, therefore, not be appropriate for realistic evaluations of tornado/downburst impacts on civil infrastructure. Very limited information is available on the temporal and spatial variations of HI wind loads for buildings (van de Lindt 2012). There are no design guidelines available in either the Canadian or other international building codes and standards. In a recent research meeting, July 2012, organized by NIST (National Institute for Standards and Technology, US), leading Canadian and US researchers identified the lack of large scale HI wind load evaluation methods as a top priority research need.

As indicated earlier, the other notable gap in wind research is perhaps generation of realistic but simple boundary conditions for sustainable built-environment or building or component design. Such designs entail consideration and integration of climate responsiveness and resilient design/retrofit of neighbourhoods, building forms, building envelope and structural systems. Therefore a clear understanding and realistic modelling of the complex interaction between the climate and the built-environment is a prerequisite. This necessitates unprecedented urban climate modelling (such as wind) at high temporal and spatial resolution. In addition sustainable systems must withstand the climate loads they are subjected to and match service life performance expectations.

To fill some of these gaps and to cope up with these challenges researchers at Western have developed a unique three-dimensional hexagonal wind testing chamber, WindEEE Dome, which can be configured to produce different flow types including straight flows, shear flows, downbursts and tornados. Similarity researchers at FIU have developed a hurricane testing facility generically named Wall of Wind. This paper discusses some salient features of these two facilities and provides various application examples.

2. Large-scale Testing Facilities

2.1 **Wall Wind**

Wall of Wind is a new full-scale hurricane testing facility at International Hurricane Research Center, Florida international University, Miami, FL. This new 12-fan WoW facility was designed to achieve target sustained wind speeds of up to 62.3 m/s (140 mph) across a 5.9 m wise by 4.3 m high (19.5 ft wide by 14 ft high) wind field for a test-specimen with a characteristic length of 3.33 m (11 ft). Provisions for generating higher wind speeds (Category 5 or more) through additional contraction modifications were considered during the design phase, and may be achieved for specialized testing and demonstrations. To house the WoW systems, a 30.5 m × 24.4 m × 10.7 m (100 ft × 80 ft × 35 ft) building was constructed. The North and South ends of the building consist of large gable end doors that will remain open during operation/testing. The WoW will be located near the South end of the build-ing. A dynamically controllable turntable, measuring 4.9 m in diameter, will allow simulation of wind effects from any direction**.**

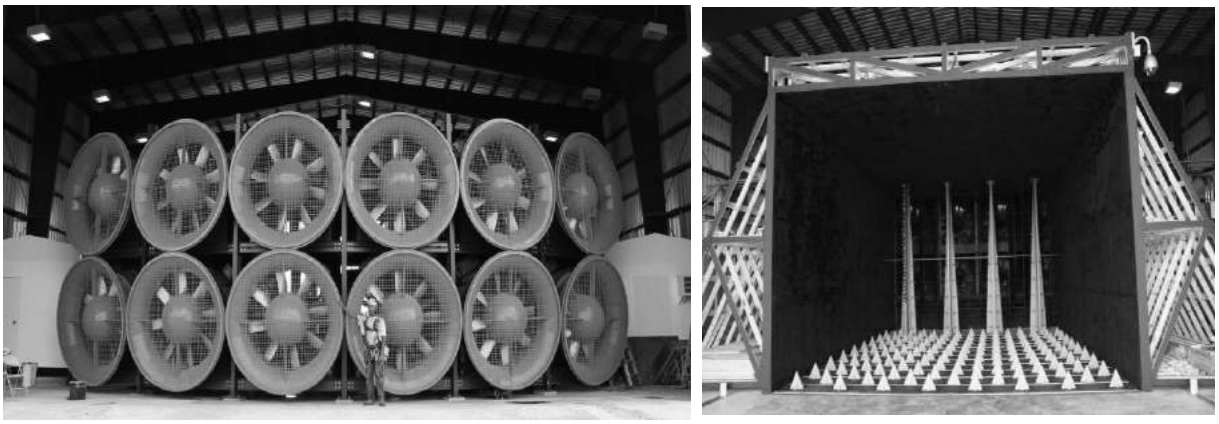

(a) **(b)**

Figure 1: Wall of Wind (a) upstream view and (b) downstream view

2.2 WindEEE Dome

The WindEEE Dome (Figure 2a) is a three dimensional wind tunnel capable of generating various types of wind systems including hurricane, tornado, downburst, sheared flow and multi-scale straight atmospheric boundary layer flows. The WindEEE Dome makes use of 106 individually controlled fans in varying configurations to achieve these flows. In a straight flow mode sixty of these fans, placed on one single wall in a matrix of 15 x4 fans are equipped with a system for gusting the fans at up to 1Hz. The inner hexagonal test chamber is approximately 25m wall to wall (Figure 2b), with 1600 floor roughness elements to control the boundary layer and a 5m diameter turntable in the centre (Figure 2c). The WindEEE Dome is configurable in both closed and open loop circuits. Up to seven operational scenarios are standard for WindEEE (see Figure 3); straight flows with large test section (Figure 3a), straight flows with high wind speed (Figure 3b), multi-phase flows (wind-driven-rain or -snow) large-scale testing (Figure 3c), tornado flows with translation (Figure 3d), downburst flows with translation (Figure 3e), and shear flows (Figure 3f). The open loop circuit and exterior platform allows for wind driven rain testing and testing of large scale test objects which would otherwise not fit inside WindEEE. In the axisymmetric mode WindEEE uses 8 fans at the bottom of each of the six walls which when coupled with other 6 fans above the ceiling level through a bell-mouth can generate tornadoes or downbursts. Using a guillotine system at the ceiling level the bell mouth translates the tornadoes and downbursts at approximately 2m/s over 5 meters inside the facility. The fully constructed WindEEE Dome at a total cost of $34M (Figure 2a) is now fully operational and is in the final stages of commissioning and flow development. WindEEE Dome represent a next generation wind engineering tool for resilient and sustainable infrastructure is expected to address some of the gaps identified earlier.

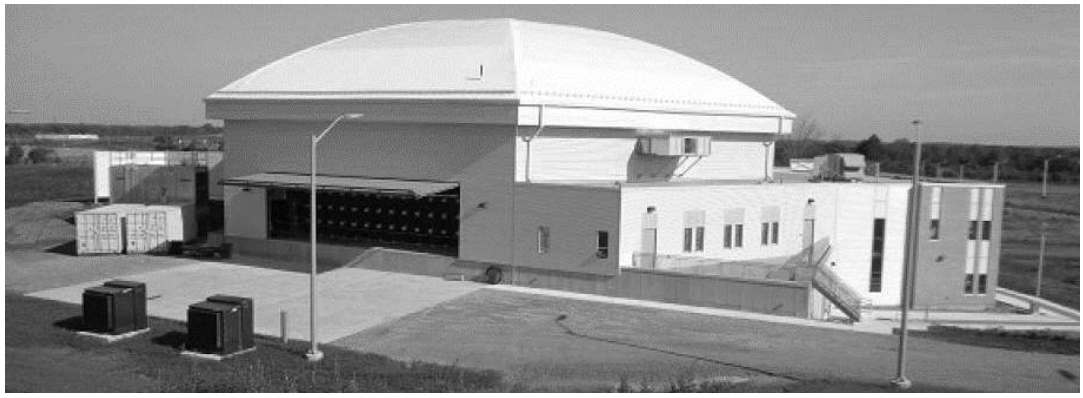

(a)

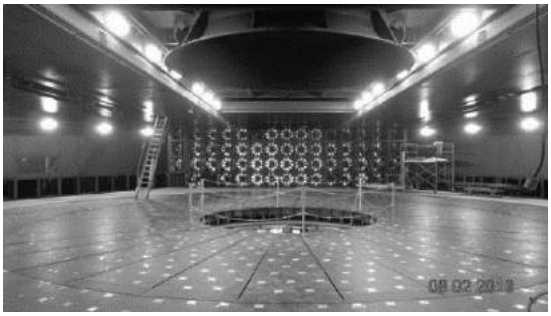

(b)

(c)

Figure 2: (a) WindEEE Dome, (b) WindEEE test chamber and (c) ground roughness elements on the test chamber floors.

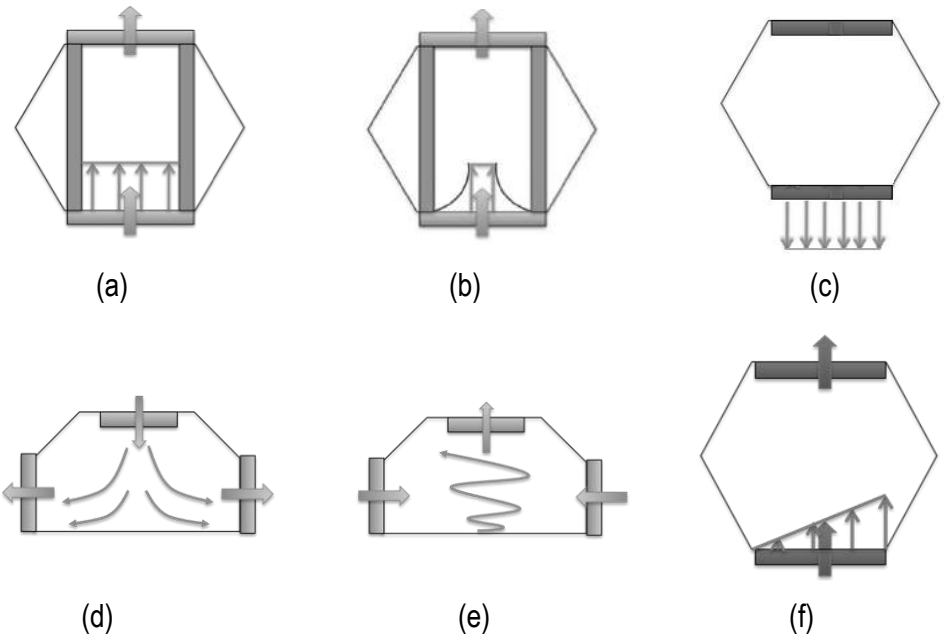

(a) (b) (c)

(d) (e) (f)

Figure 3: Six operational scenarios for WindEEE Dome: a) straight flows –large test section, b) straight flows –high speed test section, c) straight flows - multi-phase flows (wind-driven-rain or -snow) large-scale testing, d) downburst flows with translation, e) tornado flows with translation and (f) shear flows.

3. "Full"-scale Wind Testing Application Examples

3.1. Introduction

Full-scale structural wind loading information during hurricanes and severe windstorms are sparse due to the irregular occurrence and unpredictable nature of the storms. Limited full-scale wind loading from field measurements exist in the literature, but were recorded under wind conditions much lower than design-level (Levitan and Mehta 1992; Hoxey and Richards 1993; Tieleman et al. 1996). Nevertheless, studies conducted based on these field measurements, e.g., in Aylesbury (Eaton and Mayne, 1975), Silsoe (Hoxey and Richards, 1993), Lubbock (Levitan and Mehta, 1992), and by Cook et al. (1988) have provided valuable findings, and contributed to the validation or otherwise of certain wind tunnel techniques. Recently, however, several new large- and full-scale testing approaches have been (or are being) developed that are capable of testing infrastructure models with actual construction materials and at high wind speeds/forces.

Some of the full-scale facilities for testing building models include "Three Little Pigs" at the University of Western Ontario (Kopp et al. 2010), "Cyclone Testing Station" at James Cook University in Australia (http://www.jcu.edu.au/cts/), "Wind Simulator" of the University of Florida (Salzano et al. 2010), and the new full-scale facility constructed by Institute of Business and Home Safety (Liu et al. 2011). Some useful wind load data have also been collected on roofs of residential homes during hurricanes through the Florida Coastal Monitoring Program (FCMP) (Balderrama et al. 2011). Zisis et al. (2011) also studied wind load transfer mechanisms on a low wood building using full-scale load data. The WindEEE Dome, is expected to widely reinforce these efforts owing to both its size and wind speed (it can produce low level hurricane category wind speed in a test area of 5 m by 4 m) or (it can produce a large low wind speed test section of size14 m by 4 m). More exceptionally it can generate up to 5m core radius tornado and larger downbursts that can completely engulf buildings constructed in the range of 1:100 scale.

Most wind engineering experimental studies are traditionally carried out at low wind speed testing a small sized models (i.e. by using large geometric scaling factors) in a BLWT for straight winds. While there are very numerous areas of application for wind tunnel based studies as they continue to be very useful and they are widely accepted by the industry, some unresolved issues still exist. These include situations where there is a Reynolds number mismatch for structures with curved/rounded surfaces. Evidence that Re affects aerodynamics of bodies with sharp edges was also obtained from tests in pressurized wind tunnels (Larose, D'Auteuil 2006, 2008) and more recently at the Wall of Wind. Large-scale testing facilities with a high test wind speed and large test specimen are capable of achieving Reynolds numbers that are closer in magnitude to that for natural atmospheric flows in high wind events. WindEEE Dome, for example, has the capacity to manipulate a 60 fan wall (each with characteristic dimension equal to 1m) over 14 meters in width and 4 meters in height to create larger scale surface layers or even flow structures resulting from the interaction of buildings and the incoming wind (e.g separation-reattachments)

Another advantages of full-scale testing is prototype replication and measurement accuracy: The existence of architectural features such as balconies, soffits, shingles, roof pavers and roof tiles in prototype buildings are difficult to replicate in small-size models, but it can easily be accommodated on large- and full-scale building models. In addition, full-scale building models may effectively capture the intricate flow separation, vortex generation, and flow re-attachment phenomena that occur around and downwind from building edges. Testing large prototype or full scale objects in at Wall of Wind for example allows to make a step forward from overall aerodynamic loads to the measurement of stresses in individual components at high resolution.

Full-scale facilities also allows carrying out destructive testing to study failure mode mechanisms. Testing on large- and full-scale models to the point of wind-induced failure may provide a realistic assessment of the structural capacity of various construction materials and techniques. Destructive testing may provide insight to failure modes, leading to alternative designs, improved attachment methods, and appropriate mitigation techniques to enhance structural integrity and reduce losses. It has also unique practical advantages to the industry as it test the actual product and to the student as it shows directly the failures and advantageous of mitigation technologies.

3.2. Wind Load on Roof Tiles

It is a widely common seen during post damage assessments roof tiles fail. But tile aerodynamics is perhaps the least studied and has locally different aerodynamics than the global roof aerodynamics. A recent study by Tecle et al. (2013) carried out a full scale measurement of two different 'field tile' profiles, namely High profile (HP), Medium Profile (MP) among others on a gable roofed low-rise building at the Wall of Wind facility. Additionally, 'rounded' and 'three-sided' ridge tiles were also tested for a low-rise building that is 2.74 m long, 2.13 m wide and 2.13 m high. Figure 4 presents the test building in front of the older version of the Wall of Wind and some of the ridge tile types used for the study.

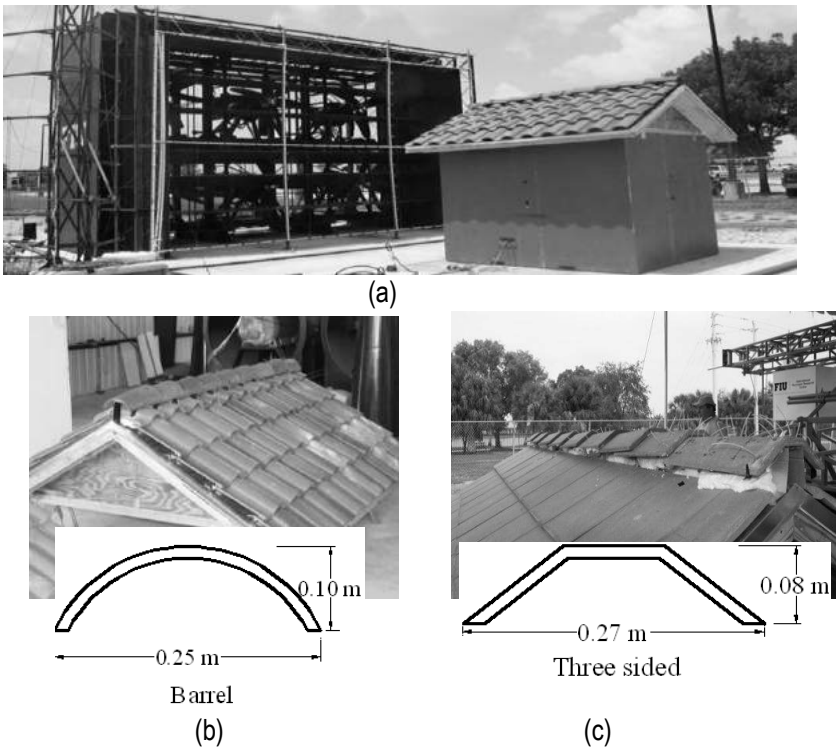

Figure 4. (a) Test specimen in front of the older version of Wall of Wind (AoA =0^0); (b) Barrel type ridge tile; (c) three-sided type ridge tile (after Tecle et al., 2013)

Six rows of pressure taps were placed on the external surface of the ridge tiles, with each row having 7 taps (Figure 5). In order to carry out high resolution pressure measurements, 21 transducers were placed on the edge ridge tiles, besides 4 pressure taps underneath the ridge tile to measure the internal pressure (cavity pressure). Additional details can be found from Tecle et al. (2013).

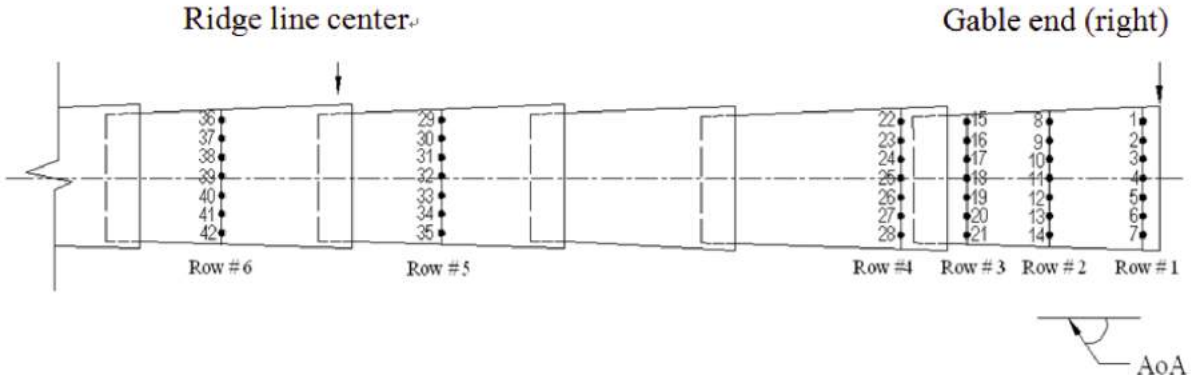

Figure 5. Pressure tap layout along the ridge line of the low-rise building (modified after Tecle et al., 2013)

The buildings were tested for 5 different Angles of Attack (AoA) of 0°, 30°, 45°, 75° and 90°. Some selected results for the ridge roof tiles are presented in Figure 6 for AoA of 0, 30 and 45 degrees since these wind angles were found to be the most critical ones.

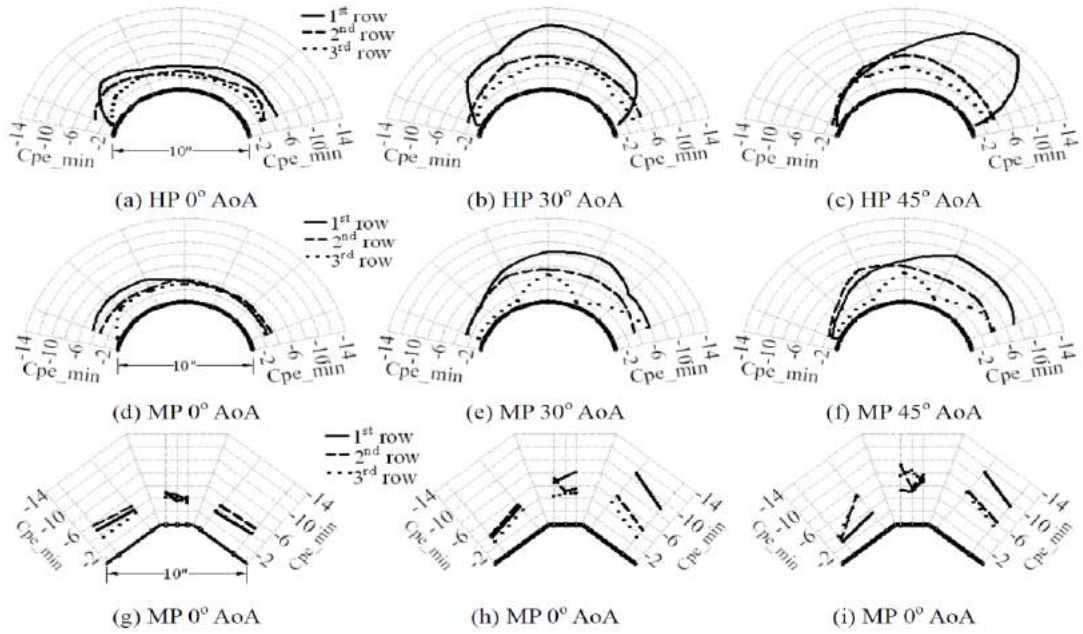

Figure 6. Pressure distributions on the ridge tiles of the low rise building with roof slope 7:12 (after Tecle et al., 2013)

Figure 6 shows that the pressure coefficients on the 1st row taps (outer row closest to the gable end) which were higher than the inner rows (2nd and 3rd rows but not shown here). The HP tile experiences high suction pressures than MP tiles at 30° (Figure 6b and e). However, at 45° the HP and MP tiles experienced comparable pressures on the wind ward side, although HP tiles experience higher pressures than the latter on the leeward side. The higher suctions on the three sided ridge is due to the sharp edges and it greater elevation above the ground at a critical AoA. These pressure coefficients on the ridge line are significantly larger (up to a factor of 5) compared to those measured on the field the roof at close location to the ridge line, for the cases considered in the study. Thus it is prudent to carry out high resolution experimental or computational studies at anticipated failure initiation locations to capture these type of hot spots that may not have been captured by the standard test procedures.

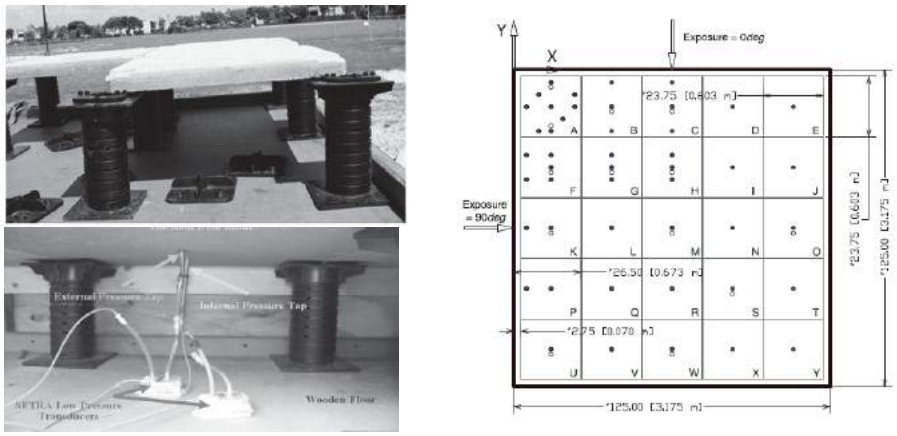

Figure 7. Paver test model detail and SETRA transducer (left) and pressure tap and paver layout (right) - solid circles designate external and hollow circles designate underneath taps (after Aly et al., 2012).

3.3. Roof Pavers

Many medium and high-rise buildings uses loosely laid roof pavers on accessible roofs. Thus avoiding any connection that could compromise the roof membrane thereby allowing rain water intrusion. However, with loosly laid pavers there could be risk of uplift from strong winds on roofs. To characterize the pressure equalization and thereby assess the effectiveness of locking the pavers together to create large balance loads, a full-scale aerodynamic test was carried out at the Wall of Wind. A full-scale test model building with 10 ft by 10 ft plan and 7 ft height dimensions was constructed and placed in a wind field of 22 ft width and 16 ft height at the Wall of Wind facility. The concrete paver is about 2 ft square in section, 1 inch thick, with 0.2 inch horizontal spacing between the pavers, and a 1 ft vertical gap between the paver and the roof deck. Figure 7a shows the roof paver test model construction. Pressure taps were installed on the upper and lower surfaces of the paver to measure external and internal (cavity) pressures using a total of 63 SETRA low pressure transducer' as shown in Figure 7b. The paver layout and location of the pressure taps are presented in Figure 7c.

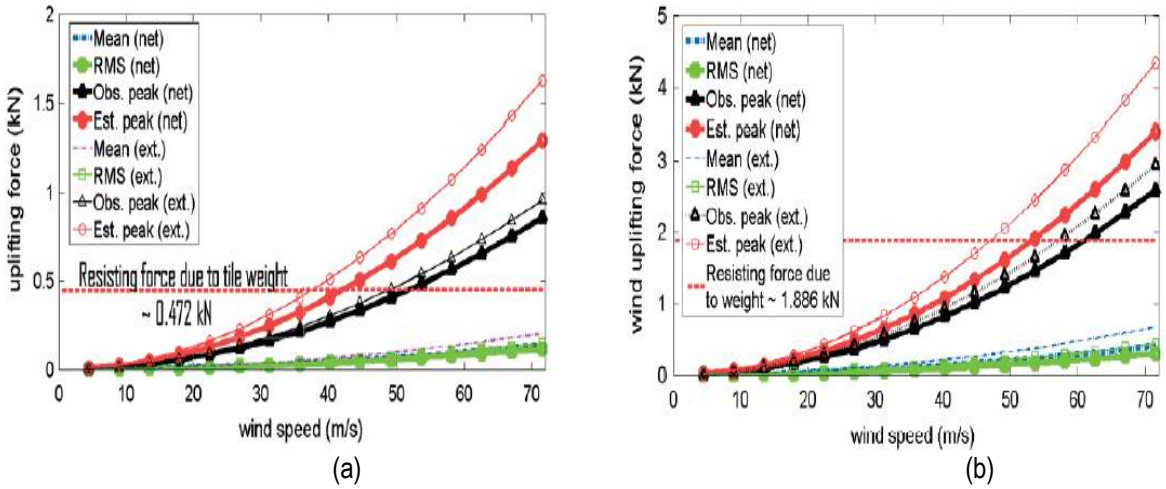

Figure 8. Wind loads acting at AoA of 67.5° on: a) Paver A (uplift force); b) Pavers A, B, F, G as a group (after Aly et al., 2013)

A selected results are presented in Figure 8a which shows mean and peak (observed and estimated) pressures on a single paver (Paver A) at 67.5° angle of attack versus wind speed and Figure 8b for the case where three tiles were locked together. It is clearly observed that an increase in wind speed also increases the wind pressures (mean and peak). Furthermore, at velocities exceeding 40 m/s, the peak pressures exceed the resisting force due to tile weight. It was found by locking the tiles the resistance to uplift increases to those corresponds to a 54 m/s wind. There are many interesting aerodynamic phenomenon in roof pavers. The first is the pressure equalization where the flow system that creates suction on the upper surface also sucks the air in the cavity (underneath the pavers) and causing cavity suction, this results in pressure equalization. The magnitude of the equalization is dependent on the several parameters such as the horizontal spacing between the tile and the vertical cavity height etc. It is to be noted that locking the pavers together, not only increases the balance weight but also decreases the overall wind load due to increased effective area (i.e. reduced pressure correlation with increased effective area achieved due to locking of many pavers together).

3.3. Roof Top Equipment

Rooftop equipment such as air-conditioning systems are a common feature of most roofs in high velocity wind zones and their failure has caused considerable damage to the building enclosure. Sometimes, the roof top equipment may get also blown off from the rooftop and damage neighboring buildings or cause human injuries that may sometimes be fatal (Erwin et al., 2011). Large scale wind testing facilities are ideal for evaluating wind load in such equipment. Figures 9a to 9e shows the test model that consists an actual Roof Top Equipment where each of the legs are mounted on a large six degree of freedom force balance (Figure 9b and 9c) that was tested for

various test configuration (Figure 9e) and wind directions. More details are provided by Erwin et al. 2011 and 2012.

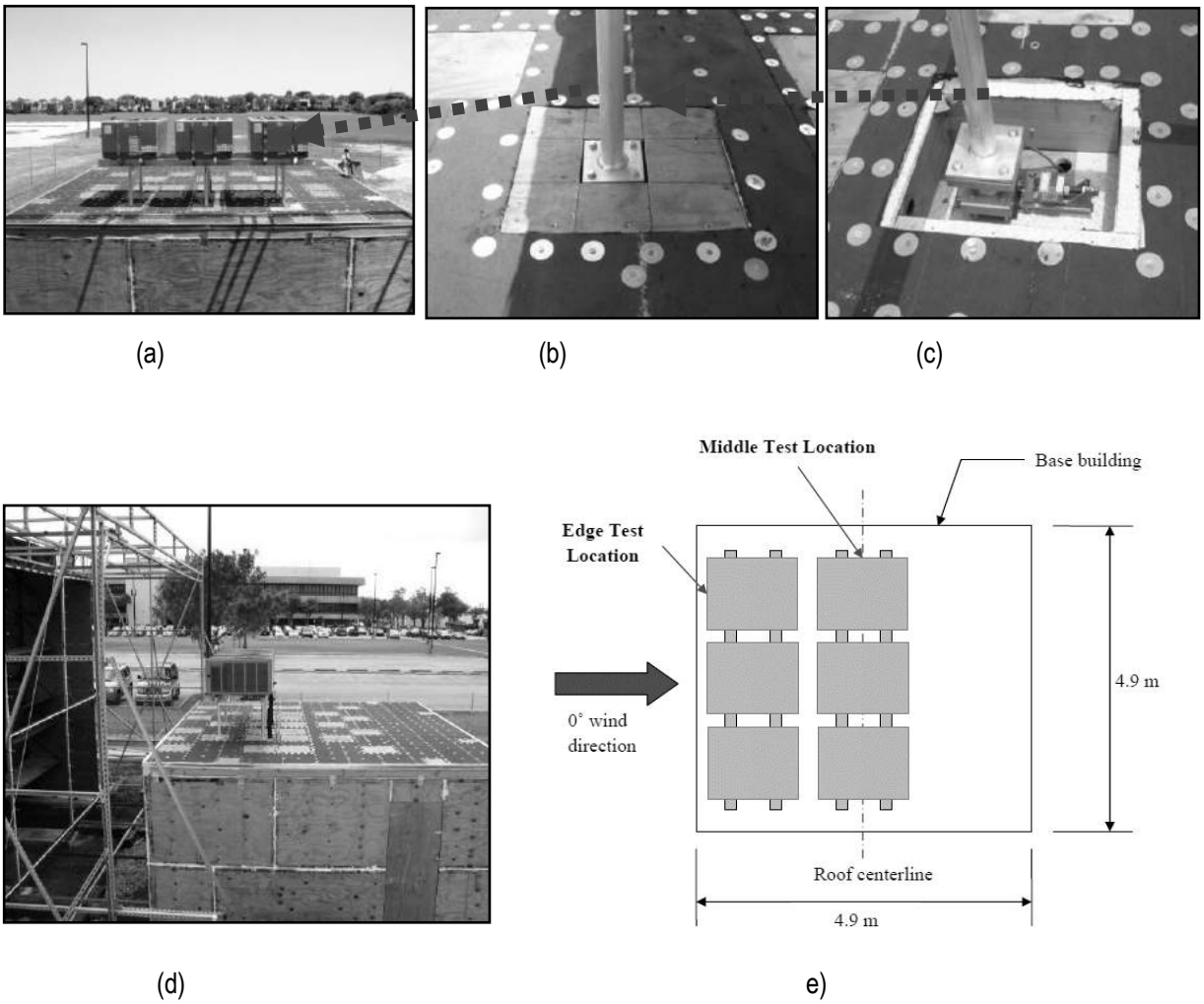

Figure 9. (a to c) Full scale rooftop equipment test model detail, (d) test model in front of the Wall of Wind and (e) plan view indicating test location configurations (after Erwin et al., 2011)

3.5 Aerodynamics of trees

With increased urbanization, there has been an increase in temperatures within the city causing urban heat island effects. As a result, many buildings adopt a sustainable design approach by having vegetated roofs (called 'green roofs') or vegetated walls, balconies etc. These are expected to reduce the temperature within the building envelope in order to provide better thermal comfort to the occupants. However, the trees could be damaged by wind causing wind born debris etc. As part of understanding the aerodynamic characteristics of trees under high velocity wind a study was carried out at full-scale at the Wall of Wind for various species of trees. Figure 10 shows a photograph of one of the tree tested at Wall of Wind at 0, 13, 26 and 40 m/s speeds. The trees changes their shape to favorably alter aerodynamic forces primarily by bending and aligning the branches and leafs flexibly in the wind direction thus effectively reducing the drag (frontal) area. As designers, perhaps we should keep learning from nature and design buildings that adapt to some extent to reduce the effect of climatic loads.

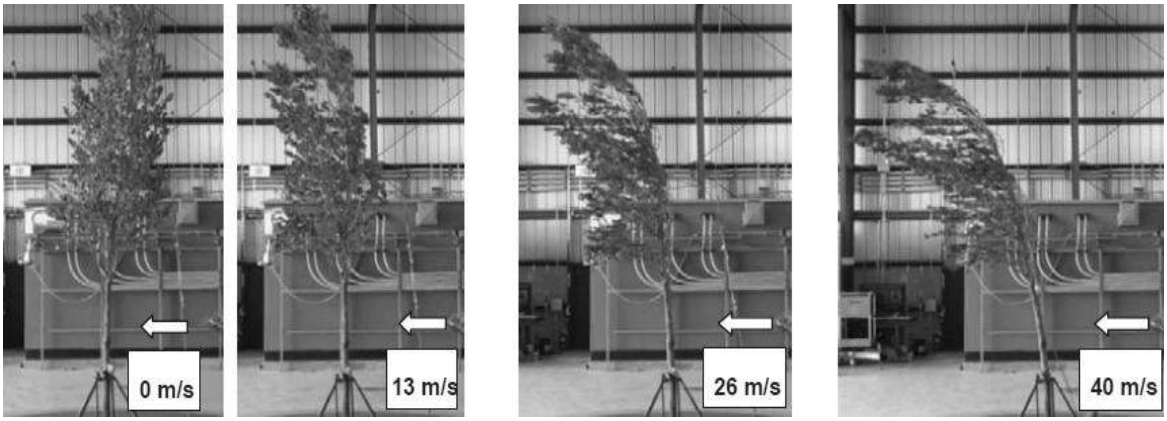

Figure 10. Photographs of the actual trees tested at the Wall of Wind at different wind speeds (modified after Aly et al., 2013)

The drag coefficient for two configurations i.e. trees without a mitigation cable (w/o) and trees attached to a mitigation cable (w) has been provided in Figure 11a. The total force coefficient was measured for different wind speeds as shown in Figure 11a for two different species of trees. The drag area is defined as shown in Figure 11b. It is very interesting to notice the reduction of the drag force coefficient with velocity increase due to tree shape adaptation as explained earlier (and as shown in Figure 12), these areoeslatic effects are very difficult to study at small scale. Aly et al. (2013) also reported that no resonance or vortex shedding was visually observed. The tree leaves/branches reduced the creation of a coherent vortex shedding and dampened all kinds of potential instability, and tree flexibility allowed significant deflections without failure.

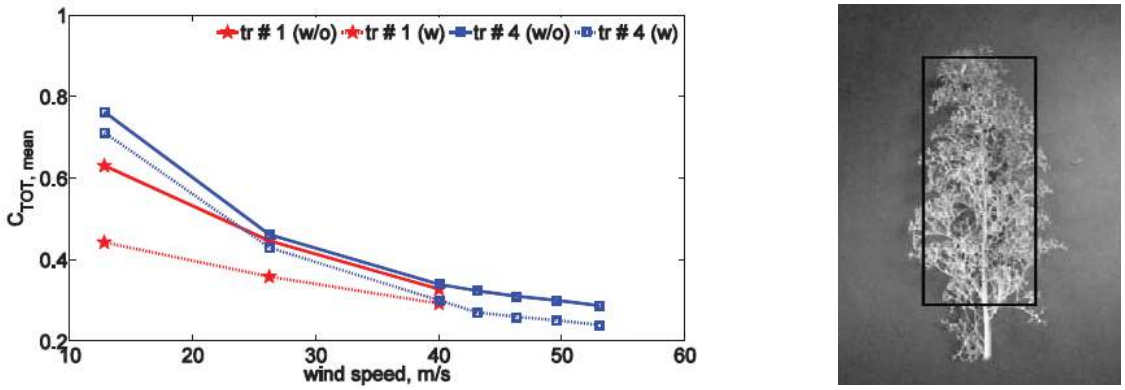

(a) (b)

Figure 11. (a) Mean total force coefficient versus wind speeds for tree 1 and tree 4, with mitigation (w) and without mitigation cable (w/o) and (b) area definition used in force coefficient calculation (modified after Aly et al., 2013)

3.6. Full-scale ground and roof mounted solar array

A new level of full-testing is being achieved at WindEEE Dome owing to its large size, reversible flow, and multi-fan system with full individual fan control capability. For example the ground mounted full-sale solar array shown in Figure 12b was tested multiple times at the WindEEE representing both ground and roof mounted solar array, without the need to have the full scale building for the latter. An attempt was made to reproduce only the flow structure above the roof level (see Figure 12a) at the WindEEE Dome. The target flow profile was obtained from PIV measurement of Kopp et al. (20xx) in standard BLWT test (Building + solar array). At the WindEEE an attempt to produce only the flow structure above the roof level was mad by utilizing WindEEE's multi-fan and reversible flow generation capability. The lower row of fans at WindEEE were run in reverse direction while the upper rows

fires the wind towards the solar panel. By trial and error the flow above the roof level was produced on the floor level of the WindEEE, thus reproducing the roof flow bubble at the WindEEE floor. Thus, by only changing the inflow boundary conditions at the WindEEE, the floor mounted solar array can be tested for various configurations representing (i) standard ABL flow or (ii) flows above roof level etc.

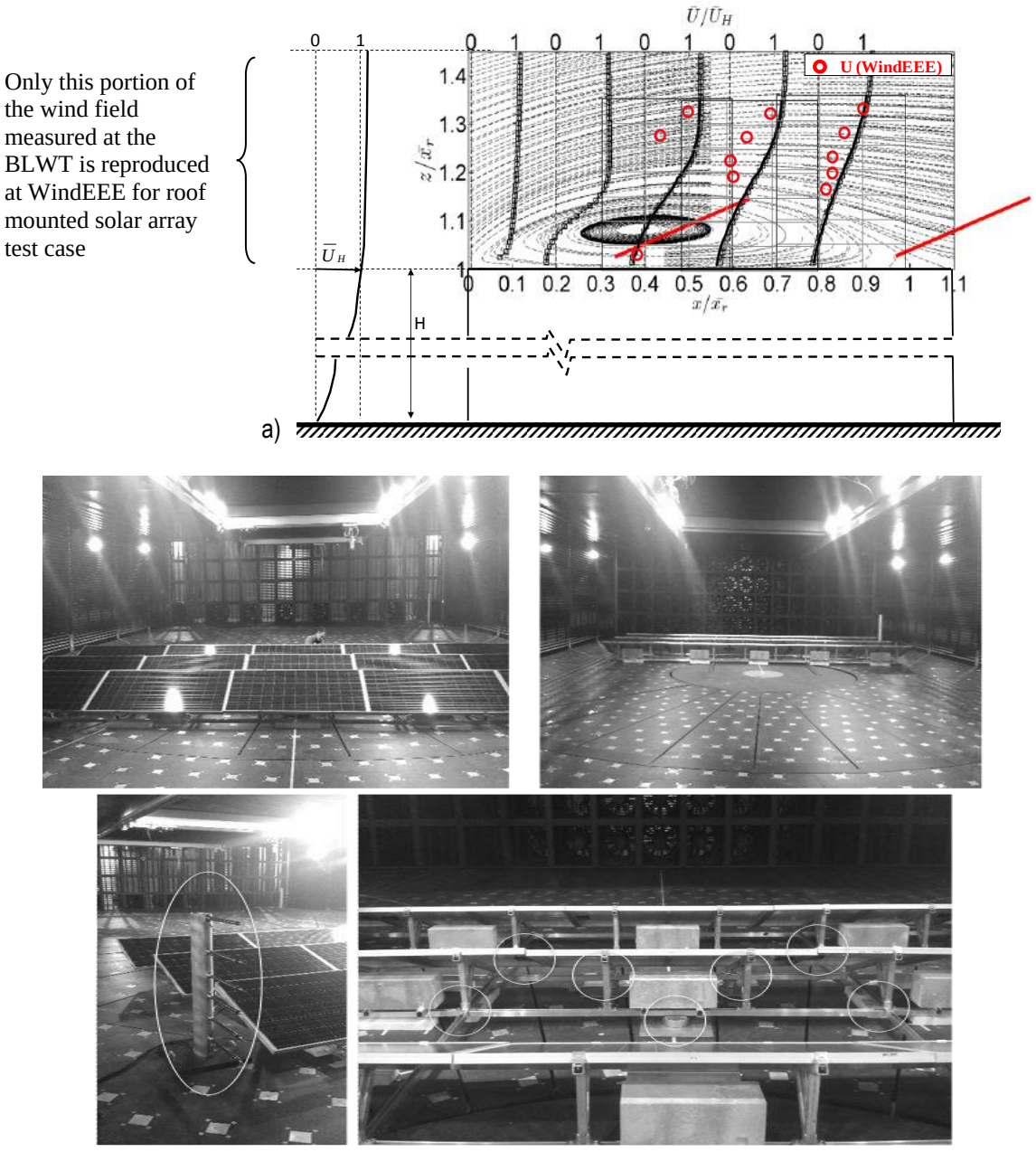

Figure 12. (a) Flow structure on flat roof, (b) full-scale solar array test set up at the WindEEE Dome.

4. Wind Driven Rain Testing Development and Application

4.1. Introduction

Post-storm damage assessment reports repeatedly have shown that the major portions of losses are due to damages on low-rise residential buildings, including building damages and consequential living expenses. A very significant portion (50 to 100%) is caused due to internal damages. However, most wind engineering studies,

including post damage assessment, focus mostly on external damages. The main source of interior damage in building is due to intrusion of rain water through breaches of the building envelope caused by large wind pressure differences and wind-borne debris. There is lack of a holistic high intensity wind–driven rain intrusion testing methodology that accounts for real construction materials and details. Recently Bitsuamlak et al. (2009) developed a large-scale high intensity wind-driven-rain intrusion testing protocol, that consists of pressure measurements (to explain water intrusion mechanisms) and developed novel but simple methods of quantifying wind-driven water intrusion. The application was demonstrated through water intrusion assessment of various types of roof secondary water barriers (described in Section 4.2 in more detail) and various roof vent openings including gable end, goose neck, turbine, ridge and soffits. Salzano et al. 2010 studied high intensity wind-driven-rain intrusion through windows. But their study was limited at a component level. Similar efforts has been carried out at the Institute for Business and Home Safety in North Carolina as well. Bahiru et al. (2014) developed wind-driven-rain generation that accounts for correct rain-drop size distribution. Following similar procedure, the WindEEE wind-driven testing on the outside platform of the 60-fan wall (14 by 4 m) allows testing of low rise buildings constructed using actual construction material and details, as it will engulf the test building completely under the wind and wind-driven-rain field more closely mimicking an actual storm..

4.2. Wind-driven-rain simulation method

According to Inculet, 2001, three key parameters need to be considered while simulating WDR on a laboratory scale, and these include model and prototype (full-scale) similarities in: (a) Reynolds number (Re); (b) Froude number; and (c) Density of water to air ratios.

The Froude number between full scale (fs) and model scale (ms) can be written as:

$$(\frac{V_r^2}{gD})_{fs} = (\frac{V_r^2}{gD})_{ms} \; or \; \lambda_v = \sqrt{\lambda_L} \qquad (1)$$

where D is the diameter of thr rain drop; V_r is the relative velocity of the rain drop; λ_v and λ_L are the velocity and length scales respectively, where $\lambda_v = (V_{ms}/V_{fs})$ and $\lambda_L = (D_{ms}/D_{fs})$.

Therefore, using the above relation and equation 1, Reynolds number for full scale $(Re)_{fs}$ and model scale $(Re)_{ms}$ can be related as:

$$(Re)_{ms} = \lambda_v^3 (Re)_{fs} \qquad (2)$$

Generally, for hurricanes the Reynolds number varies from 10^2 to 10^5, while drag coefficients vary from 1.057 to 0.45 (Foote and Toit, 1969; Morsi and Alexander, 1972). The volume of rain water per unit volume of air and its rate of deposition onto the building surface are factors affecting the WDR impact on buildings. The rain drop size distribution is defined as the ration of the number of rain drops of a particular size N (D) per unit volume of air and velocity of rain drops (Baheru et al., 2014). The number of rain drops in model scale N_{ms} and full scale N_{fs} are related with the length scale, λ_L as:

$$N_{ms} = N_{fs}/\lambda_L^4 \qquad (3)$$

Disdrometer and tipping bucket rain gauges are used in measuring WDR. The plan and elevation views of the Wall of Wind are shown in Figures 13a and 13b, while a schematic representation of the nozzle arrangement in the WoW is shown in Figure 13c. The WoW facility consists of 12 fans arranged in a 2-row by 6-column pattern to generate a wind field that is 6 m wide and 4.25 m high. A TEEJET nozzle type (TeeJet catalogue, 2011) was used corresponding to a “very coarse” rain drop size (range of 0.349-0.428 mm diameter) based on the TeeJet catalogue. According to the instrument catalogue, the number of nozzles per spray line can be found from :

$$Number\ of\ nozzles = \frac{fRR_v A}{Q_{nozzle}} \qquad (4)$$

where RR_v is the vertical rain rate; A is the vertical cross sectional area covered by the spray line; Q_{nozzle} is the volumetric flow rate through the nozzle; f is a factor that accounts for the loss in water between the nozzle location and test section. Using equation 4, 3 appropriate nozzles per spray line was determined for the Wall of Wind.

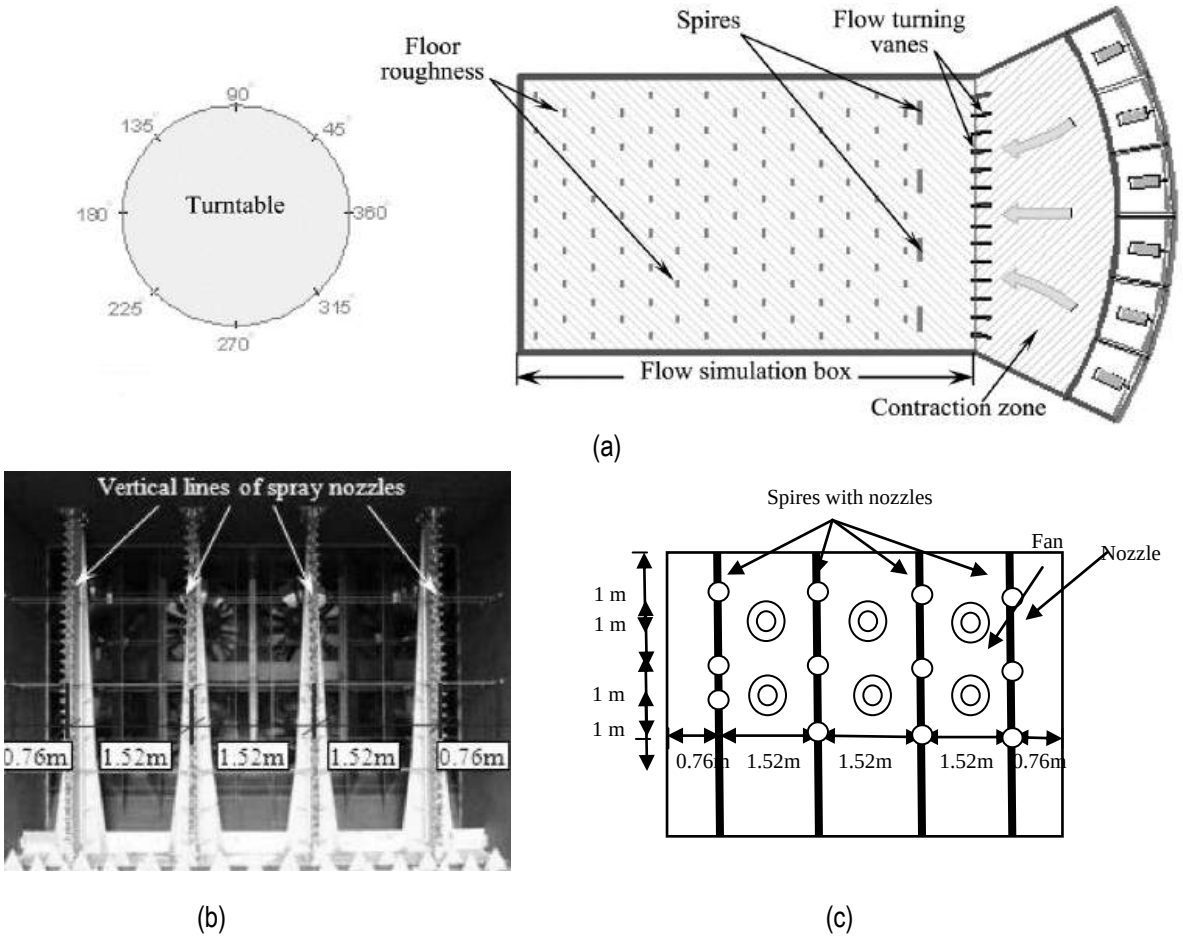

Figure 13. 12-fan Wall of Wind facility at Florida International University, USA: (a) Plan view of the facility; (b) elevation showing vertical lines of spray nozzles, (c) Schematic of the WoW facility (not to the scale) and nozzle arrangement (after Baheru et al., 2014 but modified)

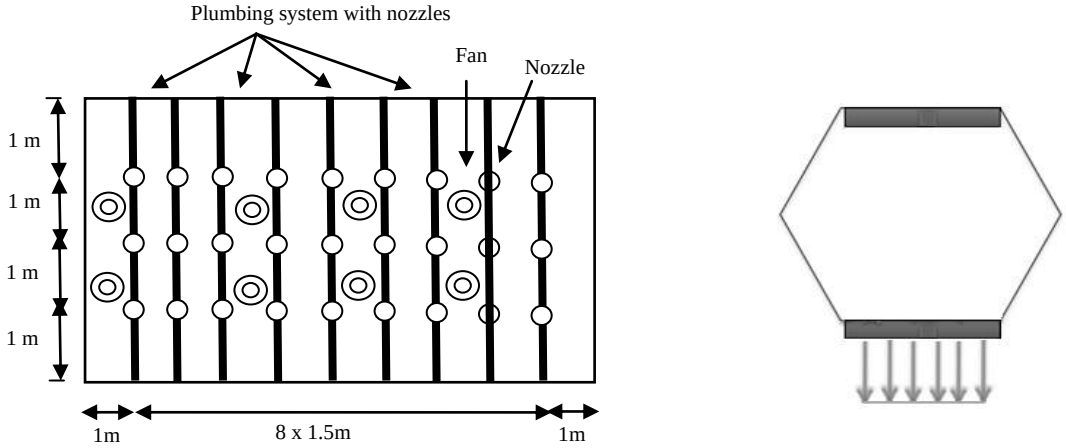

Figure 14. Schematic drawing designed WDR testing arrangement (not the scale) at the WindEEE

A similar technique was designed and is being implemented to simulate WDR at the recently constructed WindEEE facility (see Figure 14) in front of the 60 fan wall of WindEEE with a frontal section of about 14 m length and coincidentally has a height of about 4 m, similar to the Wall of Wind facility.

4.3. Wind intrusion through secondary roof membrane

As an application example, the work by Bitsuamlak et al. (2009) is presented. Their work demonstrated a holistic water intrusion test for assessing the effectiveness of roof secondary water barriers where the amount of intruded water was quantified and used as a performance index. In parallel, aerodynamic measurements were recorded and used to explain water intrusion mechanisms. Figure 15 shows the camera setup with plastic ceiling, beside the water collection procedure using buckets from the roof of the building. The tests were conducted for 3 minutes at a constant wind speed of 55 mph and turbulence intensity of 25 % (measured at 10 ft above the ground) for all test cases. Representative data is shown in Figure 16 for rain intrusion through different types of secondary water barriers, which include asphalt and synthetic based barriers for light, self adhered and heavy types.

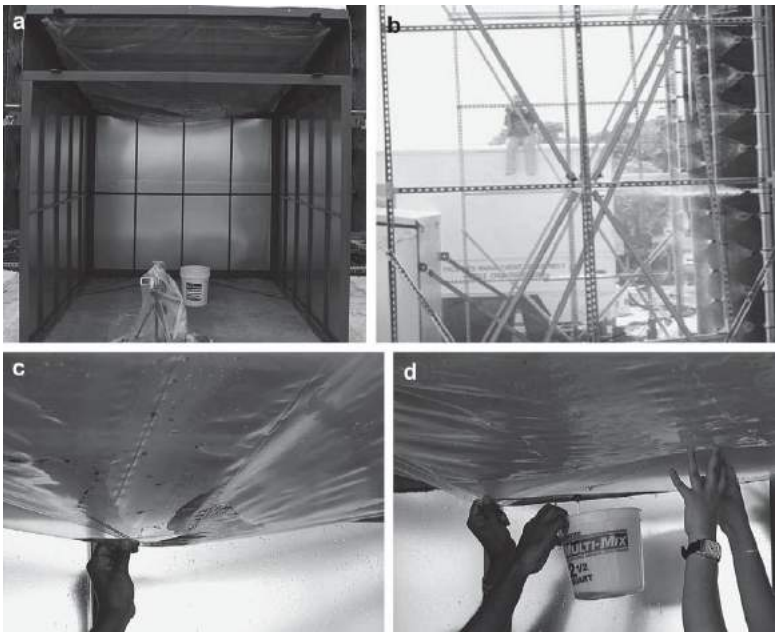

Figure 15. Water monitoring and collection setup: (a) Complete setup with camera and plastic ceiling, (b) the SWB test specimen from bird's view and (c) leaked water through the roof layer and (d) water collection (after Bitsuamlak et al., 2009).

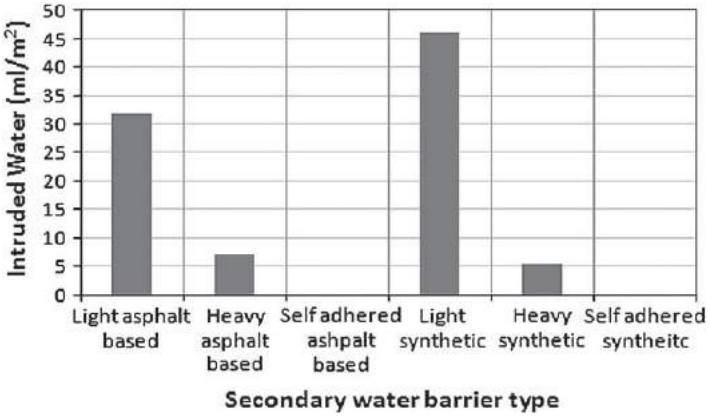

Figure 16. Water intrusion for various water barrier types (after Bitsuamlak et al., 2009)

Results show greater intrusion (about 75 % higher) through lighter asphalt than the heavier asphalt water barrier. Higher wind speeds allow greater accumulation of water on the slope, intruding the overlap created by suction resulting in water leaking to the plywood underneath. Similar observations were made for light synthetic water barriers as opposed to the heavy synthetic type, where the former produced almost 90 % more water intrusion than the latter. In fact, the water intrusion in buildings causes significant damage, as shown in Figure 18.

5. Summary

This paper presents the new approaches in Wind Engineering that focus on "Full"-scale wind and wind-driven-rain testing. Two such facilities the Wall of Wind and WindEEE Dome were presented. Various full-scale application presented. These tools are expected to enable the wind engineering community address problems that were not possible through the use traditional low-wind speed and small size facilities.

6. References

1. Abdi, D. and Bitsuamlak, G.T. 2014. Numerical evaluation of the effect of multiple roughness changes. In publication by Wind and Structures.
2. Aboshosha, H., Bitsuamlak, G.T and El Damatty, A. Turbulence characterization of downbursts using LES, Accepted for publication Journal of Wind Eng. & Industrial Aerodynamics.
3. Aly, A.M, Fossati, F, Muggiasca, S, Argentini, T, Bitsuamlak, G, Franchi, A, Longarini, N, Crespi, P, Chowdhury, A.G. 2014. Wind loading on trees integrated with a building envelope. Wind and structures, 17, 69-85.
4. Aly, A.M., Bitsuamlak, G.T. 2013. Aerodynamics of ground-mounted solar panels: test model scale effects. Journal of Wind Engineering and Industrial Aerodynamics. 123(a), 250-260.
5. Aly A.M., Bitsuamlak, G.T., Gan Chowdhury, A. 2012. Full-scale aerodynamic testing of a loose concrete roof paver system. Engineering Structures. 44, 260–270.
6. Baheru, T., Gan Chowdhury, A., Bitsuamlak, G.T., Masters, F.J., Tokay, A. 2014. Simulation of wind-driven rain associated with tropical storms and hurricanes using the 12-fan Wall of Wind. Building and Environment. 76, 18–29.
7. Balderrama, J.A., Masters, F.J., Gurley, K.R., Prevatt, D.O., Aponte-Bermúdez, L.D., Reinhold, T.A., Pinelli, J.-P., Subramanian, C.S., Schiff, S.D., Chowdhury, A.G. 2011. The Florida Coastal Monitoring Program (FCMP): A Review. J. Wind Eng. Ind. Aerodyn., 99(9), 979-995.
8. Bitsuamlak, G.T., Gan Chowdhury, A., Sambare, D. 2009. Application of full-scale testing facility for assessing wind-driven-rain intrusion. Building and Environment. 44(12), 2430-2441.
9. Bitsuamlak, G.T., Stathopoulos, T., Bédard, C. 2005. Effect of upstream hills on design wind load: a computational approach. Wind and Structures. 9(1), 37-58.
10. Castillo, L., Seo, J., Hangan, H. and Johansson, G. 2004. Smooth and rough turbulent boundary layer at high Reynolds number. Experiments in Fluids. 36(5), 759-774.
11. Cochran, L. 2006. Review Article: State of the art review of wind tunnels and physical modeling to obtain structural loads and cladding pressures. Architectural Science Review, 49, 7-16.
12. Cook, N. J., Keevil, A. P. & Stobart, R. K. 1988. BRERWULF—the big bad wolf. J. Wind Eng. Ind. Aerodyn. 29, 99–107.
13. Dagnew, A., Bitsuamlak, G.T. 2014. Computational evaluation of wind loads on standard tall building using a large eddy simulation. In publication by Wind & Structures.
14. Dagnew, A., Bitsuamlak, G.T. 2012. Computational evaluation of wind loads on buildings: A review. Wind and Structures. 16(6), 629-660.
15. Eaton, K.J. and Mayne, J.R. 1975. The measurement of wind pressures on two storey houses at Aylesbury. J. Wind Eng. Ind. Aerodyn.1, 67-109.
16. Erwin, J, Gan Chowdhury, Bitsuamlak, G.T. 2011. Rooftop equipment wind load and mitigation techniques, Journal of Wind Engineering, 8 (1), 23-42.
17. Erwin, J, Chowdhury, A.G, Bitsuamlak, G.T. 2012. Full Scale and Wind Tunnel Testing of Rooftop Equipment on a Flat Roof. Advances in Hurricane Engineering, (doi: 10.1061/9780784412626.049), pages-553-560.

18. Gan Chowdhury, A., Bitsuamlak, G., Simiu, E. 2010. Aerodynamic, hydro-aerodynamic, and destructive Testing. ICE Structures and Buildings Journal, 163 (SB2), 137-147.
19. Haan, F., Sarkar, P.P., Gallus, W. 2008. Design, construction and performance of a large tornado simulator for wind engineering applications. Engineering Structures. 30, 1146-1159.
20. Hangan, H. 2014. The Wind Engineering Energy and Environment (WindEEE) Dome, Wind Engineers, JAWE, Vol 39, No 4 (No. 141), October 2014.
21. Hashemi-Tari, P., Gurka, R, Hangan, H. 2010. Experimental investigation of tornado-like vortex dynamics with Swirl Ratio: The mean and turbulent flow fields . J. Wind Eng. Ind. Aerodyn. 98 (12), 936-944.
22. Holmes, J.D., Hangan, H., Schroeder, J.L., Letchford, C.W. and Orwig, K.D. 2008. A forensic study of the Lubock-Reese downdraft of 2002. Wind and Structures. 11, No. 2, 137-152.
23. Hoxey, R.P. and Richards, P.J. 1993. Flow patterns and pressure fields around a full-scale building. J. Wind Eng. Ind. Aerodyn. 50, 203-212.
24. Inculet. D.R. 2001. The design of cladding against wind driven rain, University of Western Ontario, Canada.
25. Kim, J.D., Hangan, H. 2007. Numerical characterization of impinging jets with application to downbursts. J. Wind Eng. Ind. Aerodyn. 95(4), 279-298.
26. Kopp, G.A., Morrison, M.J., Henderson, D.J. Full-scale testing of low-rise buildings using realistically simulated wind loads. 13th ICWE, Key note paper, Amsterdam, Netherlands, 2011.
27. Kopp, G., Morrison, M., Gavanski, E., Henderson, D., and Hong, H. 2010. Three Little Pigs" Project: Hurricane Risk Mitigation by Integrated Wind Tunnel and Full-Scale Laboratory Tests. Nat. Hazards Rev., 11(4), 151–161.
28. Larose, G.L., D'Auteuil, A. 2008. Experiment on 2D rectangular prisms at high Reynolds numbers in a pressurized wind tunnel. J. Wind Eng. Ind. Aerodyn. 96, 923-933.
29. Larose, G.L., D'Auteuil, A. 2006. On the Reynolds number sensitivity of the aerodynamics of bluff bodies with sharp edges. J. Wind Eng. Ind. Aerodyn. 94, 365-376.
30. Letchford, C.W., Mans, C., Chay, M.T. 2002. Thunderstorms, their importance in wind engineering - a case for the next generation wind tunnel. J. Wind Eng. Ind. Aerodyn. 90, 1415-1433.
31. Levitan, M.L. and Mehta, K.C. 1992. Texas Tech field experiments for wind loads. Part I: Buildings and pressure measurement system. J. Wind Eng. Ind. Aerodyn. 41-44, 1565-1576.
32. Liu, Z., Brown, T.M., Cope, A.D., Reinhold, T.A. Simulation wind conditions/events in the IBHS research center full-scale test facility. 13th ICWE, Amsterdam, Netherlands, 2011.
33. Matsui, M., Tamura, Y. "Influence of swirl ratio and incident flow conditions on generation of tornado-like vortex. 5th European and African Conf. on Wind Eng., Florence, Italy, July 19-23 2009.
34. Mishra, A. R., James, D. L., Letchford, C. W. 2008. Physical simulation of a single-celled tornadolike vortex, Part A: Flow field characterization. J. Wind Eng. Ind. Aerodyn. 96(8), 1243-1257.
35. Mishra, A. R., James, D. L., Letchford, C. W. 2008. Physical simulation of a single-celled tornadolike vortex, Part B: Wind loading on a cubical model. J. Wind Eng. Ind. Aerodyn. 96(8), 1258-1273
36. Nasir, Z., Bitsuamlak, G. Similarities and differences among tornadic and synoptic flow induced loads on a bluff-body, Engineering Mechanics Institute Conference, Hamilton, Ontario, Canada, August 5-8, 2014.
37. Nasir, Z., Bitsuamlak, G., Hangan, H. Computational modeling of tornadic load on a bluff-body, 6th International Symposium on Computational Wind Engineering, Hamburg, Germany, June 8-12, 2014.
38. Natarajan, D., Hangan, H. 2012. Large eddy simulations of translation and surface roughness effects on tornado-like vortices. J. Wind Eng. Ind. Aerodyn. 104-106, 577–584
39. Prevatt, D., van de Lindt, J., Back, E., Graettinger, A., Pei, S., Coulbourne, W., Gupta, R., James, D., and Agdas, D. 2012. Making the Case for Improved Structural Design: Tornado Outbreaks of 2011. Leadership Manage. Eng. 12(4), 254–270.
40. Rajasekharan, G.S., Matsui, M. and Tamura, Y. 2012. Dependence of surface pressures on a cubic building in tornado like flow on building location and ground roughness. J. Wind Eng. Ind. Aerodyn. 103, 50-59.
41. Selvam, P., Millet, P. 2003. Computer modeling of tornado forces on buildings. Wind & Structures, 6(3), 209–220.
42. Tamura, T., Nozawa, K., Kondo, K. 2008. AIJ guide for numerical prediction of wind loads on buildings. J. Wind Eng. Ind. Aerodyn. 96, 1974-1984

43. Salzano, C.T., Masters, F.J. and Katsaros, J.D. 2010. Water penetration resistance of residential window installation options for hurricane-prone areas. Building and Environment, 45(6), 1373-1388.
44. Tecle, A., Bitsuamlak, G.T., Suksawang, N., Gan Chowdhury, A., Feuze Lekem, S. 2013. Ridge and field tile aerodynamics for a low-rise building: a full-scale study. Wind & Structures, 16(4) 301-322.
45. TeeJet. 2011. TeeJet technologies catalogue, 51, Wheaton, Illinois, USA.
46. Tieleman, H.W., Surry, D., Mehta, K.C. 1996. Full/model-scale comparison of surface pressures on the Texas Tech experimental building. J. Wind Eng. Ind. Aerodyn. 61(1–23), 1–23.
47. van de Lindt, J., Pei, S., Dao. T., Graettinger, A., Prevatt, D., Gupta, R., and Coulbourne, W. 2012. A dual-objective-based Low-rise tornado design philosophy. ASCE J Struct Eng, 139(2), 251–263.
48. Zisis, I. and Stathopoulos, T. 2011. Wind load transfer mechanisms on a low wood building using full-scale load data. 13th International Conference in Wind Engineering, Amsterdam, Netherlands.
49. Xu, Z. and Hangan, H., Scale, boundary and inlet condition effects on impinging jets with application to downburst simulations, J. of Wind Eng. and Ind. Aerodynamics, 96, 2383–2402, 2008.